

AutoWS-Bench-101: Benchmarking Automated Weak Supervision with 100 Labels

Nicholas Roberts* Xintong Li* Tzu-Heng Huang Dyah Adila
Spencer Schoenberg Cheng-Yu Liu Lauren Pick Haotian Ma
Aws Albarghouthi[†] Frederic Sala

University of Wisconsin
{nick11roberts, aws, fredsala}@cs.wisc.edu,
{xli2224, thuang273, adila, spencer.schoenberg, cliu547, lpick2, hma232}@wisc.edu

August 31, 2022

Abstract

Weak supervision (WS) is a powerful method to build labeled datasets for training supervised models in the face of little-to-no labeled data. It replaces hand-labeling data with aggregating multiple noisy-but-cheap label estimates expressed by labeling functions (LFs). While it has been used successfully in many domains, weak supervision’s application scope is limited by the difficulty of constructing labeling functions for domains with complex or high-dimensional features. To address this, a handful of methods have proposed automating the LF design process using a small set of ground truth labels. In this work, we introduce **AutoWS-Bench-101**: a framework for evaluating automated WS (AutoWS) techniques in challenging WS settings—a set of diverse application domains on which it has been previously difficult or impossible to apply traditional WS techniques. While AutoWS is a promising direction toward expanding the application-scope of WS, the emergence of powerful methods such as zero-shot foundation models reveals the need to understand how AutoWS techniques compare or cooperate with modern zero-shot or few-shot learners. This informs the central question of AutoWS-Bench-101: given an initial set of 100 labels for each task, we ask whether a practitioner should use an AutoWS method to generate additional labels or use some simpler baseline, such as zero-shot predictions from a foundation model or supervised learning.¹ We observe that in many settings, it is necessary for AutoWS methods to incorporate signal from foundation models if they are to outperform simple few-shot baselines, and AutoWS-Bench-101 promotes future research in this direction. We conclude with a thorough ablation study of AutoWS methods.

1 Introduction

The success of modern deep learning has been driven by large labeled datasets. Unfortunately, obtaining labeled data at scale is expensive and slow. Weak supervision (WS) [1, 2, 3, 4] is one of the most successful solutions to the problem of generating labeled datasets. The idea behind WS is simple: replace hand-labeling with acquiring and aggregating noisy-but-cheap label estimates from external sources—also called labeling functions (LFs)—to produce denoised estimates of true labels. WS is deployed widely and has had a significant impact. For example, in the medical domain, it has been used to re-create radiography datasets in a few hours that saved physician-months in manual labeling costs [5]. It has led to the creation of the largest dataset of aortic valve malformations developed atop the large-scale UK Biobank [6, 7]. In addition, WS has enjoyed wide industrial adoption. It is used in production by core teams within Google, Apple, and many more [8, 9].

Despite its massive success and widespread adoption, weak supervision can be challenging to apply. While much cheaper than manually labeling millions of examples, LF generation is sometimes costly. Obtaining high-quality LFs often requires training domain experts and painstaking iteration. Furthermore, creative choices must be made when applying WS to new modalities. For example, LFs that apply to text may not lift to image segmentation [10] or recommendation [11] tasks.

* Equal contribution

[†] Author’s name in native alphabet: أوس البرغوثي

¹The goal of generating the 101st label onward gives our benchmark its name.

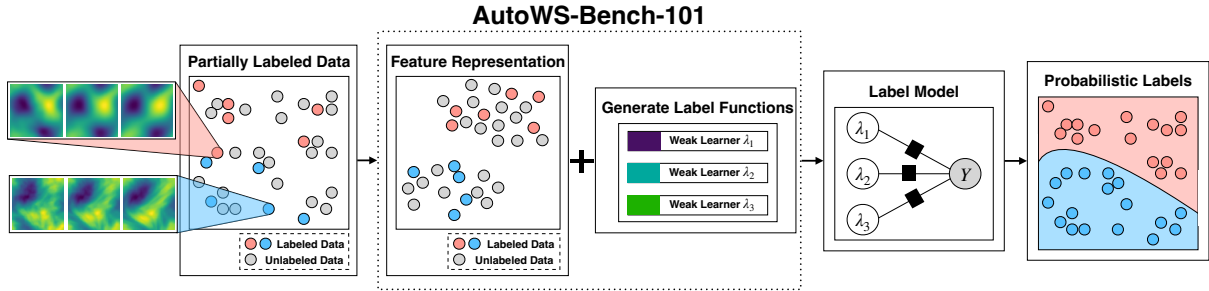


Figure 1: Overview of the AutoWS-Bench-101 pipeline.

Automated WS (AutoWS) methods are a best-of-both-worlds solution. These techniques generate LFs automatically by training models on a small initial set of ground truth labels [12, 13, 14]. At first glance, AutoWS techniques resemble few-shot learners. However, they are much more, forming *omnivorous frameworks* capable of incorporating and combining signals from many sources, including powerful few- and zero-shot models. Indeed, recent evidence [15, 16] suggests that WS can exploit signal from powerful foundation models like CLIP, GPT-3, and T0++ [17, 18, 19].

AutoWS techniques have tremendous potential. For example, they

- can fuse multiple sources of signal, including foundation models, to maximize performance,
- inherit from WS the ability to denoise labels and to generalize beyond their constituent LFs,
- enable applying WS to domains and modalities where hand-crafting LFs is difficult or impossible.

Missing, however, is a thorough comparison of AutoWS techniques or an in-depth understanding of which components lead to good performance. For example, intuitively these methods rely on high-quality feature representations, but it is not clear how performance scales with the choice of representation. It is crucial to understand how these methods compare to—and can be combined with—existing few- or zero-shot models. Motivated to understand these mechanics under a diverse data settings previously underexplored by WS, we propose **AutoWS-Bench-101**.

AutoWS-Bench-101 is a framework and benchmark for experimenting with, understanding, and evaluating AutoWS methods. It enables plug-and-play combinations of feature representations, LF candidate generation approaches, and LF selection procedures, conveniently built on top of the WRENCH [20] framework. It can be used with existing AutoWS methods like Snuba [12], interactive WS [13], and GOGGLES [14], or extensions of such techniques. A pipeline is shown in Figure 1. AutoWS-Bench-101 evaluation uses a diverse set of datasets on which WS has previously seen little application. Our benchmark reveals the following key insights about AutoWS:

1. Foundation models **are only helpful to AutoWS for in-distribution or related tasks**,
2. LFs that output multiple classes **might be better than class-specialized LFs**,
3. Foundation model usage can **hurt coverage**, the fraction of points labeled by AutoWS.

Once AutoWS methods are better understood, these methods have the promise of drastically increasing the application scope of WS. Our benchmark takes a crucial first step toward this understanding. We publicly release all experiment code and datasets for AutoWS-Bench-101 on GitHub.²

2 Background

We provide background on weak supervision (WS), automated WS (AutoWS), along with pretrained and foundation models. Finally, we formalize the background on AutoWS by providing a mathematical formulation of the problem setting.

Weak Supervision WS methods generate labels for unlabeled data by combining multiple sources of imperfect label estimates [1, 2, 4, 11]. These easily obtained and applied sources are called labeling functions (LFs). They can be created from heuristic rules produced by an expert, knowledge-base queries, pre-trained model outputs, or by any other means cheaper than obtaining ground-truth labels [21, 22, 23, 24, 25]. LFs provide a noisy estimate of the label, or otherwise abstain. If all the LFs abstain on a point, WS methods cannot label it; the fraction of points labeled by WS is the *coverage*.

Much of the WS literature focuses on the label model, the tool used to aggregate LF outputs to produce de-noised label estimates. New variants with different properties were introduced in [1, 3, 4, 11]. The recent benchmark

²<https://github.com/Sala-Group/AutoWS-Bench-101>

WRENCH [20] focuses on evaluating such models. In contrast, we are focused on understanding the mechanics of AutoWS independent of the choice of label model.

Automated Weak Supervision In many cases, the process of designing LFs is expensive or challenging. Several automated weak supervision (AutoWS) methods have been developed to automatically create LFs from some small initial set of labeled examples. Snuba [12] generates a large set of weak learners trained on combinations of features and iteratively selects LFs based on various performance criteria. Interactive Weak Supervision (IWS) [13] also selects LFs from a pool of candidates by interactively learning from human feedback. While not explicitly an automated procedure, IWS is easily modified to not require a human in the loop. Finally, GOGGLES [14] was introduced to address the challenge of automating the LF creation process, as well as the challenge of using WS for image data. GOGGLES computes pairwise affinity scores between feature representations of examples obtained by, for example, a pretrained VGG16 network, and learns a hierarchical generative model on the resulting affinity matrices. Additionally, several AutoWS methods have been developed specifically for the NLP domain. Some methods such as Darwin [26], PRBoost [27], and Nemo [28], like IWS, query annotators for feedback to assess the quality of synthesized rules. Other frameworks can be more complex and even more tailored to the NLP domain, such as ARI, which integrates inferred rules into pretrained NLP models [29].

Pre-trained and Foundation Models Powerful pre-trained models are increasingly useful in modern machine learning. A standard approach to sidestep acquiring huge labeled datasets is to fine-tune a pre-trained model. For image data, this might be a ResNet [30] trained on ImageNet. Self-supervised models [31, 32] can be used to acquire high-quality representations enabling users to train a simpler downstream model using fewer labeled points. Foundation models [33], large-scale models trained on vast amounts of data, can be used as few- or zero-shot predictors. These approaches can be thought of as either competitors of AutoWS—if used as alternatives—or as AutoWS *ingredients*. For example, WS can be performed on top of foundation model embeddings, or use them to extend LF coverage [15], or use prompts as sources [16]. Understanding how pre-trained or foundation models compete with or contribute to AutoWS is a key element of this work.

Problem formulation We provide a mathematical formulation of the AutoWS problem setting here. First, we begin with an unlabeled training set of n examples $X_{\text{train}} = [x_i]_{i=1}^n$ with $x_i \in \mathcal{X}$ and a labeled validation set of m examples $X_{\text{val}} = [x_j]_{j=n+1}^{n+m}$ with $x_j \in \mathcal{X}$, $Y_{\text{val}} = [y_j]_{j=n+1}^{n+m}$ with $y_j \in \mathcal{Y}$. Next, we embed examples in \mathcal{X} into \mathbb{R}^d using a feature extractor, which we denote as $\phi : \mathcal{X} \rightarrow \mathbb{R}^d$. Additionally, we denote the hypothesis class of synthetic LFs as \mathcal{H} where $\forall h \in \mathcal{H}$, we have $h : \mathbb{R}^d \rightarrow \mathcal{Y} \cup \{-1\}$. We will denote an AutoWS method as a pair of algorithms, the first of which generates LFs and is parameterized by a feature extractor: $\mathcal{A}_{\text{WS}}^\phi = (\text{LF}_{\text{WS}}^\phi, \text{LM}_{\text{WS}})$ where $\text{LF}_{\text{WS}}^\phi : \mathcal{X}^{n+m} \times \mathcal{Y}^m \rightarrow \mathcal{P}(\mathcal{H})$ and the second is the label model, which infers a weak label from one or more LF predictions: $\text{LM}_{\text{WS}} : \mathcal{Y}^{\geq 1} \rightarrow \mathcal{Y}$. We generate LFs using $\Lambda = \text{LF}_{\text{WS}}^\phi(X_{\text{train}}, X_{\text{val}}, Y_{\text{val}})$ and obtain LF predictions $\forall h_k \in \Lambda$ as $\lambda_i^k = h_k(\phi(x_i))$. We can furthermore obtain additional label predictions for each example from other sources, such as zero-shot predictions from foundation models or by using hand-designed LFs. We will denote the set of these additional predictions as $\tilde{\lambda}_i = \left\{ \tilde{\lambda}_i^l \right\}_{l \geq 0}$, $\forall i \in [n+m]$. Finally, we obtain weak labels for the training set using the label model: $\hat{y}_i = \text{LM}_{\text{WS}}(\{\lambda_i^k\}_{k=1}^{|\Lambda|} \cup \tilde{\lambda}_i)$, $\forall i \in [n]$. In this work, we evaluate choices of ϕ and $\mathcal{A}_{\text{WS}}^\phi$.

3 Benchmark Goals and Methodology

We describe the goals of our proposed benchmark and our experimental methodology.

Goals The goal of this work is to understand the effects of the key components of AutoWS—LFs, selection methods, and representations—on a diverse collection of datasets. We are especially interested in settings far from the ambit of conventional weak supervision—most often used in text applications. We also seek to understand how AutoWS compares to leading zero-/few-shot methods when used as either an alternative or an ingredient.

Methodology For ease-of-use, our benchmark is implemented as an extension of the recently introduced Weak supeRvision BENCHmark (WRENCH) [20]. We note that WRENCH and AutoWS-Bench-101 have fundamentally different goals: WRENCH evaluates label models, not AutoWS techniques. An additional difference is that WRENCH uses fixed pre-computed LFs and only includes a handful of image-based datasets without access to the original source images or videos.

We consider three well-known methods for generating LFs: Snuba, IWS, and GOGGLES [12, 13, 14], operating on a handful of baseline features: raw pixels, PCA with 100 principal components, the logits layer of a pre-trained ResNet-18 [30], and zero-shot logits from CLIP [17]. The AutoWS-Bench-101 pipeline is shown in Figure 1. Below, we explain our choices in more detail.

3.1 Datasets

In order to evaluate AutoWS techniques on a range of challenging WS settings, we include a diverse set of 10 classification datasets. Image classification datasets are a salient example of the types of datasets that fit our goal, as these have proven to be a challenging domain for weak supervision. We include two such datasets, MNIST and CIFAR-10 [34, 35], in AutoWS-Bench-101. We wish to avoid AutoWS methods overfitting to the image domain through the exploitation of feature representations specifically tailored to these tasks. For this reason we include two image-derived datasets that move beyond the scope of natural image classification. Spherical MNIST [36] consists of MNIST digits stereographically projected onto the sphere, rotated, and mapped back to the plane. Permuted MNIST consists of MNIST digits whose pixels are permuted by a fixed bit-reversal permutation applied to the rows and columns. We additionally include three text datasets that are also used in WRENCH [20]: YouTube [37], Yelp [38, 39], and IMDb [39, 40]. Finally, we include three tasks in more diverse application settings beyond image, image derived, or text datasets. These are the electrocardiogram (ECG) dataset of [41], a turbulence classification variant of the Navier-Stokes PDE data used in [42], and EMBER, a tabular malware detection dataset [43]. Further details of the latter three datasets are provided below.

ECG The ECG, or electrocardiogram dataset is commonly used to detect heart disease. It contains 60 second or shorter ECG recordings posed as a four-class classification problem: normal, disease, other, or noisy. This dataset was derived from the 2017 PhysioNet Challenge [41]. We use a fixed size of sliding window to process signals into a 1,000 ms time-series dataset.

Navier-Stokes The Navier-Stokes equation is a partial differential equation that describes viscous fluid flows. A property of interest to the computational fluid dynamics community is the turbulence of these flows. In the case of the Navier-Stokes equation, this is governed by a viscosity parameter η . Navier-Stokes solutions are generated by [42]. We adapt the Navier-Stokes dataset at $\eta = 1e-3$ (non-turbulent) and $\eta = 1e-5$ (turbulent) to be a binary turbulence classification task.

EMBER The EMBER dataset, or Elastic Malware Benchmark for Empowering Researchers, introduced by [43], is a tabular malware detection dataset extracted from malicious and benign Windows portable executable files. EMBER dataset is a binary classification task, and it includes several groups of feature, such as parsed features, format-agnostic features, and string information to detect malware. We use the open source implementation to extract features.³

3.2 Implementation Details

We adapt the open source implementations of Snuba, IWS, and GOGGLES to be compatible with WRENCH [12, 13, 14, 20]. As AutoWS methods require a small set of labeled examples, we use 100 labeled examples in all experiments unless otherwise stated. We include a few-shot learning baseline—a logistic regression classifier trained on the same 100 labeled examples. Additionally, we include a semi-supervised baseline—label propagation [44]. Finally, we include zero-shot CLIP as another baseline. In the final evaluation of each method, we report output label model accuracy (see Table 1) and coverage (see Appendix).

Snuba and Multiclass Snuba Unless otherwise stated, we use the Snuba implementation and hyperparameters [12]. This implementation only supports binary classification—however, five our datasets are multiclass. We adapt Snuba to multiclass settings in two ways. First, we run Snuba’s LF synthesis procedure for each class as a one-vs-all problem. This results in **unipolar** LFs—a given LF will either vote for its assigned class or abstain. We also implemented a **multipolar** version of Snuba where LFs are themselves multiclass. By default, the search space of LFs is fixed to be decision stumps, logistic regression, or nearest neighbor classifiers. We found that allowing Snuba to consider both decision stumps and logistic regression classifiers for any given LF led to a slight improvement in performance. All of our experiments consider both of these. Each LF abstains according to a confidence threshold

³<https://github.com/elastic/ember>

that is inferred by Snuba during the LF synthesis procedure. Finally, as in the original Snuba implementation, we aggregate the outputs of each LF using the label model.

Interactive Weak Supervision We adapt the original implementation of IWS to our setting. IWS operates on an initial pool of binary LFs. For simplicity, we use Snuba’s LF synthesis procedure to generate a large set of LFs that IWS can select from. Note that since we use Snuba’s LF synthesis procedure, each LF has its own inferred abstention threshold. Specifically, we generate LFs with cardinality $D = 1$, the number of features that each LF can consider. Similarly, unless otherwise stated, we consider both decision stumps and logistic regression classifiers. Like Snuba, the original IWS implementation only supports binary classification. Since our benchmark is over 10-class problems, we run the IWS LF selection procedure once per class to produce unipolar LFs for each class before passing the outputs of these to the label model.

GOGGLES GOGGLES computes pairwise affinity scores on a set of unlabeled examples which are used in a hierarchical generative model with to infer labels. To construct the affinity matrix, the default implementation uses the max-pooling layers of the pre-trained VGG-16 network to extract various levels of semantic representations. In our experiments, we replace these VGG-16 representations with our baseline feature representations. Pairwise affinity scores are computed by cosine similarity between embeddings of each instance. After training a generative model to create clusters, GOGGLES uses a small amount of labeled datapoints to map clusters to classes. Note that GOGGLES does not abstain.

CLIP We used standard CLIP [17] zero-shot prediction as a baseline, comparing image embeddings (except for the tabular dataset EMBER) with text embeddings of strings related to the class label. The complete list of these strings is provided in the Appendix.

BERT embeddings for text datasets Our pipeline requires the features of each dataset to be compatible with all (or most) of the feature representation techniques that we evaluate. In order to make the text datasets that we evaluate work with our pipeline, we first extract feature vectors for our text datasets using BERT before applying other feature representations (except in the case of CLIP, which operates on text directly). For YouTube, Yelp, and IMDb, raw features refers to these BERT features, PCA embeddings refers to the PCA of BERT features, and ResNet-18 embeddings refers to BERT features passed through a pretrained ResNet-18 model. In the case of CLIP, we directly use the CLIP text encoder for both the input text and the candidate labels to produce a logits vector.

4 Analysis

AutoWS-Bench-101 evaluates combinations of AutoWS methods and feature representation methods on a diverse set of classification tasks. Specifically, we evaluate GOGGLES, Interactive Weak Supervision, Snuba, and a multi-polar variant of Snuba using raw features, PCA, the logits layer of a pretrained ResNet-18, and CLIP logits. We compare all of these to a logistic regression-based few-shot learning baseline, and a Label Propagation-based semi-supervised baseline [44]. In order to robustly assess differences in the types of data domains under which various methods work best, we split our evaluations across image tasks (MNIST, CIFAR-10, Spherical MNIST, Permuted MNIST), diverse tasks (ECG, Navier-Stokes, EMBER), and text tasks (YouTube, Yelp, IMDb). We will go on to describe our analysis and results for determining which AutoWS and feature representation methods work well and do not work well on AutoWS-Bench-101.

4.1 Comparison methodology

In addition to presenting a full set of results in Table 1, we adopt the performance profiles methodology of [45] to summarize many of our results in a holistic manner. These are a robust way to visually compare methods in aggregate across noisy evaluations in a large number of environments (i.e., problem settings). The performance profile shows curves where points along each curve represent the fraction of settings where a given method is within a factor of the best method. This factor is denoted τ . Concretely, for each method s in a set of methods \mathcal{S} , we plot $\rho_s(\tau) = \frac{1}{|\mathcal{P}|} \left| \left\{ p \in \mathcal{P} : \frac{\text{obj}_{p,s}}{\min_{s \in \mathcal{S}} \text{obj}_{p,s}} \leq \tau \right\} \right|$, where \mathcal{P} is the set of problem settings/environments and $\text{obj}_{p,s}$ is the objective for s . The ideal curve has a high fraction, approaching the top-left corner.

The goal of AutoWS is to produce high accuracy and high coverage (that is, to label as many points as possible). When discussing accuracy, we set $\text{obj}_{p,s}$ to be standard classification error. For coverage, we set $\text{obj}_{p,s}$ to be $1 - \text{coverage}$. We set \mathcal{E} to be the set of feature representations, \mathcal{W} to be the set of AutoWS methods, and \mathcal{D} to be

	MNIST	CIFAR-10	SPHERICAL MNIST	PERMUTED MNIST	ECG	NAVIER-STOKES	EMBER	YOUTUBE	YELP	IMDB
GOGGLES										
+RAW FEATURES	0.3778	0.1697	0.0897	0.3778	0.2710	0.5284	0.5283	0.5880	0.4732	0.5516
+PCA	0.4563	0.1989	0.1074	0.4561	0.2688	0.4863	0.6728	0.5880	0.5466	0.5628
+RESNET-18	0.3258	0.1768	0.1192	0.1894	0.3127	0.9353	0.5312	0.5200	0.4553	0.5152
+CLIP	0.3309	0.5436	0.1884	0.1405	N/A	0.7505	N/A	0.5280	0.4779	0.5000
IWS										
+RAW FEATURES	0.4128	0.1482	0.1154	0.3862	0.2615	0.5403	0.4997	0.4896	0.6034	0.5478
+PCA	0.3503	0.1047	0.1283	0.4970	0.2687	0.5155	0.4777	0.5217	0.5260	0.5045
+RESNET-18	0.0822	0.2120	0.1352	0.5101	<u>0.4235</u>	0.7995	0.7343	0.7840	0.5620	0.5286
+CLIP	0.6885	0.7892	0.1108	0.3495	N/A	N/A	N/A	N/A	N/A	N/A
SNUBA										
+RAW FEATURES	0.2694	0.1624	0.0805	0.2308	0.2648	0.5235	0.7082	0.7520	0.6034	0.5936
+PCA	0.2313	0.0924	0.1526	0.2640	0.2598	0.8811	0.4905	0.6640	0.7187	0.5560
+RESNET-18	0.4219	0.1520	0.1554	0.1804	0.2506	<u>0.9774</u>	0.6994	0.7400	0.5674	0.5804
+CLIP	0.6617	<u>0.7550</u>	0.3103	0.2419	N/A	0.8414	N/A	0.6280	0.5608	0.5699
SNUBA (MULTIPOLAR)										
+RAW FEATURES	0.2374	0.1386	0.0991	0.2343	0.2596	0.5421	0.7264	0.7080	0.6484	0.6072
+PCA	0.5625	0.1390	0.2354	0.5625	0.2644	0.8968	0.5143	0.6280	0.7218	0.5020
+RESNET-18	0.3866	0.2036	0.1588	0.2283	0.3702	0.9742	0.7559	0.7320	0.5526	0.5864
+CLIP	0.3541	0.6788	0.2479	0.2785	N/A	0.7916	N/A	0.7759	0.5435	0.5681
FEW-SHOT (LOGISTIC)										
+RAW FEATURES	0.7295	0.2315	0.1496	<u>0.7295</u>	0.2583	0.6316	0.6517	0.8920	0.7871	0.6472
+PCA	<u>0.7306</u>	0.2262	0.1483	0.7305	0.2548	0.7863	<u>0.7488</u>	<u>0.8880</u>	<u>0.7868</u>	<u>0.6464</u>
+RESNET-18	0.7966	0.3335	<u>0.2544</u>	0.3485	0.4700	1.0000	0.5329	0.7000	0.5682	0.5856
+CLIP	0.3579	0.6857	0.1011	0.1009	N/A	0.7658	N/A	0.7000	0.6347	0.5636
SEMI-SUPERVISED (LABEL PROP.)										
+RAW FEATURES	0.7066	0.1927	0.1374	0.7066	0.2644	0.5010	0.5003	0.8440	0.5447	0.5812
+PCA	0.7165	0.1914	0.1405	0.7156	0.2644	0.5011	0.5003	0.8440	0.5450	0.5812
+RESNET-18	0.7124	0.1277	0.1283	0.2106	0.2644	0.9700	0.5003	0.7000	0.5224	0.5500
+CLIP	0.1178	0.5780	0.1009	0.1009	N/A	0.5058	N/A	0.6480	0.5737	0.5400
CLIP ZERO-SHOT	0.5817	0.6989	0.2065	0.0899	N/A	0.6305	N/A	0.472	0.5223	0.5008

Table 1: Test accuracies of AutoWS methods across features and datasets using 100 labels. N/A denotes an incompatibility between a method, feature representation, and/or task—see Appendix. **Bolded** and underlined scores indicate the **first** and second best results, respectively.

the set of datasets that we consider. We evaluate feature representations $\phi \in \mathcal{E}$ and AutoWS methods $\mathcal{A}_{\text{WS}}^\phi \in \mathcal{W}$ by defining their respective sets of environments to be datasets subject to either using a particular AutoWS method, or feature representation, respectively.

4.2 Comparison of feature representations and AutoWS methods

When do foundation models help AutoWS? First, we study the performance of different feature representation methods across datasets and AutoWS methods. Full results are presented in Table 1. We compare feature representation methods using performance profiles by defining an environment to be a dataset and AutoWS method pair. Specifically, we set $\mathcal{S} = \mathcal{E}$ and $\mathcal{P} = \mathcal{D} \times \mathcal{W}$. We then plot performance profile curves for each feature representation method as shown in Figure 2 (bottom row). We find that CLIP performs quite well on all of the image tasks that we evaluate, whereas ResNet-18 features and raw features were less performant compared to other methods. We postulate that this is because these tasks are somewhat similar to CLIP’s training distribution. On diverse tasks, however, CLIP performs much worse—due to its incompatibilities with certain data modalities, such as time series (ECG) and embeddings of tabular data (EMBER), and when using IWS on Navier-Stokes, where the input dimensionality (2) of is too small to generate a large number of LFs. We hypothesize that this is because Navier-Stokes is farther from CLIP’s training distribution. Surprisingly, ResNet-18 (which was pretrained on ImageNet) appears to perform quite well on diverse tasks; it achieves the best performance on ECG, and Navier-Stokes under using few-shot baseline and the best performance on EMBER when using Snuba with multipolar LFs. We hypothesize that, while aimed at handling diverse downstream image tasks, ImageNet contains enough semantic information beyond images that it can handle, to at least a rudimentary degree, diverse tasks as well. This observation is in the same vein as prior work which shows that training on (seemingly unrelated) non-linguistic data improves downstream performance on natural language tasks [46]. On text tasks, we find that CLIP underperforms, but we postulate that this is mainly due to the lack of image input in these settings. On the other hand, we find that

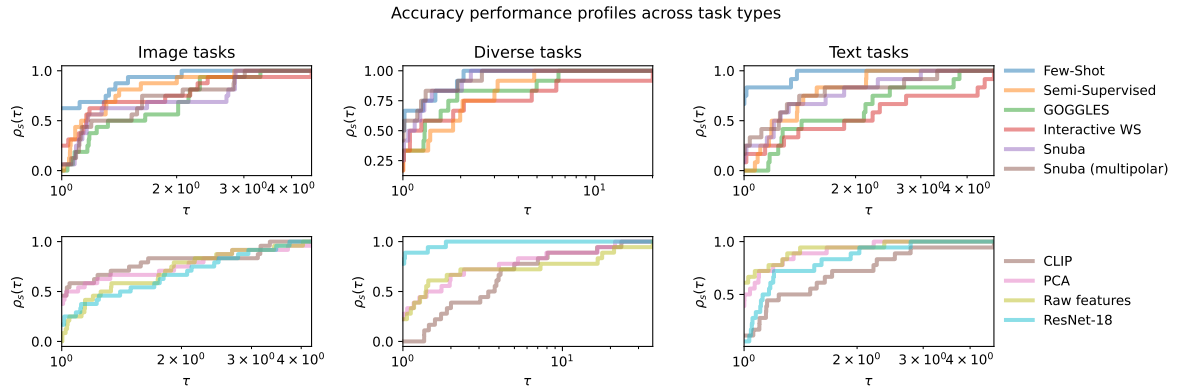


Figure 2: For image tasks (left)—MNIST, CIFAR-10, Spherical MNIST, Permuted MNIST—few-shot learning and CLIP both dominate. For diverse tasks (center)—ECG, Navier-Stokes, Ember—Snuba closes the gap with few-shot learning and CLIP underperforms or is non-applicable. For text tasks (right)—YouTube, Yelp, IMDb—few-shot learning and raw features (i.e., BERT embeddings), while the CLIP text encoder alone underperforms or faces compatibility issues with IWS.

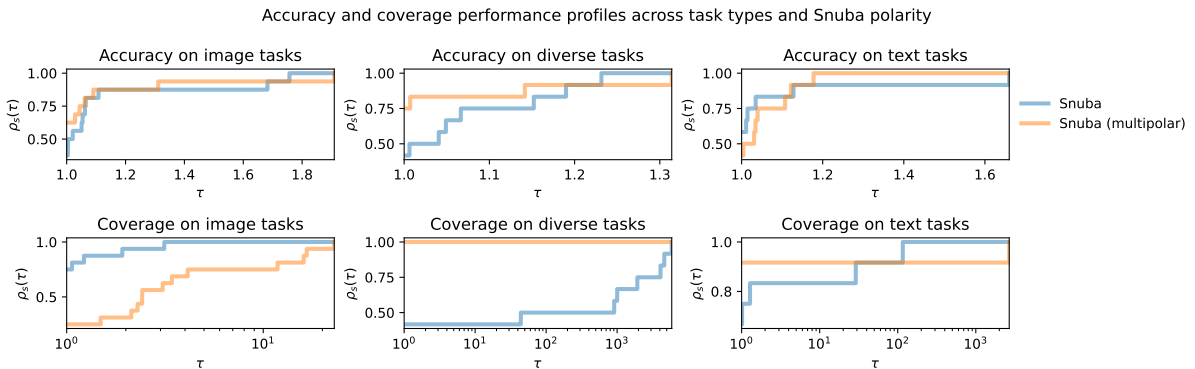


Figure 3: Using multipolar LFs typically improves the performance of Snuba (top). The difference is more pronounced on diverse tasks (top center). Multipolar LFs can result in lower coverage among image tasks (bottom left) which are notably all 10-class classification tasks. Conversely, multipolar LFs result in perfect coverage for the diverse tasks, which have fewer classes (bottom center).

raw features (i.e., text features extracted using BERT) outperforms other methods. Perhaps unsurprisingly, we find that our few-shot baseline (logistic regression) using raw BERT features outperforms all other methods on text tasks, as this corresponds to standard BERT fine-tuning, which furthermore suggests that this method should be *combined* with AutoWS methods. Our key finding is that **CLIP helps AutoWS on in-distribution image tasks or image-derived tasks. CLIP does not help on diverse out-of-distribution tasks or on tasks where only text input is available, in which raw BERT features help.**

How does AutoWS compare to few-shot learning? Next, we compare AutoWS to few-shot learning. Full results are in Table 1. For our performance profiles we set $\mathcal{S} = \mathcal{W}$ and $\mathcal{P} = \mathcal{D} \times \mathcal{E}$. The curves are shown in Figure 2 (top row). We find that few-shot learning typically outperforms any other method on image tasks, attaining strong average performance. However, we note that in terms of absolute performance, IWS and Snuba perform the best on CIFAR-10 and Spherical MNIST (both when using CLIP), though they are less robust to changes in the underlying feature representation. As shown in Figure 2 (top center), we find that Snuba (both unipolar and multipolar) perform similarly to few-shot learning on diverse tasks. On Navier-Stokes, multipolar Snuba nearly matches the 100% accuracy of the few-shot baseline and on EMBER, multipolar Snuba outperforms few-shot learning using ResNet-18 features. In terms of absolute performance on all applicable datasets, at least two of the AutoWS methods also outperform raw zero-shot CLIP predictions. We again note that for all text tasks, few-shot learning using raw BERT features (i.e., fine-tuning BERT) outperforms all other methods. Our key finding is that **few-shot learning is a strong baseline with good average performance across tasks, which suggests that it should be combined with AutoWS methods.**

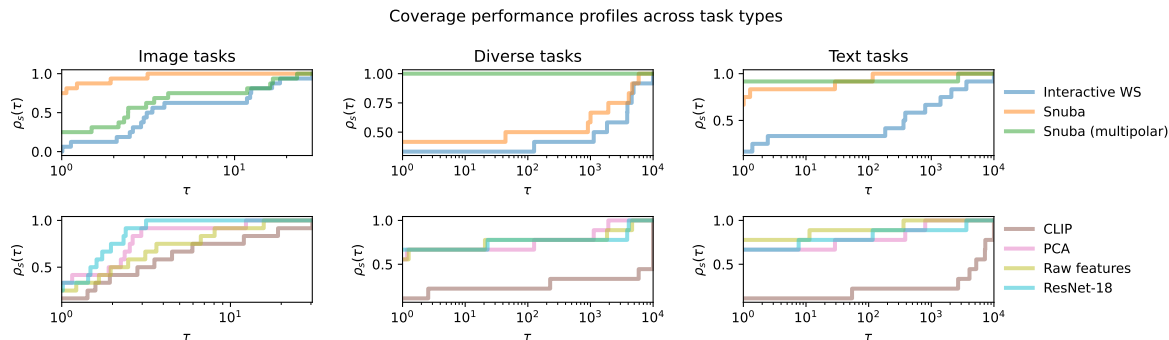


Figure 4: For image tasks (left)—MNIST, CIFAR-10, Spherical MNIST, Permuted MNIST—Snuba attains high coverage, and CLIP usage tends to worsen coverage. For non-image tasks (right)—ECG, Navier-Stokes, Ember—Multipolar Snuba always attains full coverage and CLIP is either non-applicable or attains poor coverage.

4.3 Evaluation of scientific questions using AutoWS-Bench-101

Are multiclass LFs better than class-specialized LFs? Next, we directly compare Snuba with unipolar LFs to Snuba with multipolar LFs. To our knowledge, a study of the value of unipolar vs. multipolar LFs has not been previously conducted in the WS literature. The top row of Figure 3 shows that multipolar Snuba can attain slightly better average performance than unipolar Snuba across all feature representations on image tasks, though in terms of absolute numbers in Table 1, unipolar Snuba significantly outperforms multipolar Snuba when using CLIP embeddings (typically the best feature representation for both methods). On diverse tasks, multipolar Snuba outperforms or nearly matches unipolar Snuba, across all feature representations. We furthermore find that on diverse tasks, multipolar Snuba attains perfect coverage in all cases, whereas unipolar Snuba often does not. We note that on these diverse tasks, ECG has 4 classes the other two, Navier-Stokes and EMBER, are binary. We find that on text tasks, multipolar Snuba tends to outperform unipolar Snuba subject to using the best feature representations for each. We also note that multipolar Snuba attains greater than or equal coverage to Snuba on the text tasks (which are all binary) in all but one instance—YouTube with CLIP embeddings. Surprisingly, we find that multipolar Snuba’s high coverage does not translate to image tasks, where the number of classes is higher, and unipolar LFs tend to result in much higher coverage on average. We conclude that **multipolar LFs tend to perform better on average but result in lower coverage when the number of classes increases.**

Do the best methods still cover the label distribution? A critical aspect for a WS method to be practically useful is that it must be able to produce labels for all of the classes in the label distribution with the same frequency at which they occur in the underlying data distribution. We thus perform an analysis of the coverage of methods in our pipeline subject to using different AutoWS methods and feature representations. We first consider the effect of using different AutoWS methods on coverage. We detail all of the coverage results across IWS, Snuba, and multipolar Snuba in the Appendix (note that GOGGLES by definition always produces 100% coverage). We present performance profile results of our coverage analysis in Figure 4. As before, we find that unipolar Snuba still attains the best coverage across 10-class image tasks, while multipolar Snuba attains the best coverage across diverse tasks and text tasks (with the only exception being YouTube with CLIP embeddings). In the bottom row of Figure 4, we show that methods using CLIP attain, on average, comparatively low coverage across all tasks. On diverse tasks, this can be attributed to the fact that CLIP is only applicable to Navier-Stokes, and not to ECG or EMBER (see Figure 4, bottom right). On text tasks, this is partly due to the inapplicability of 2D CLIP logits to IWS (see Appendix for a more detailed explanation of incompatibilities). However, CLIP is applicable to all image tasks, and still attains the worst coverage performance across feature representations (see Figure 4, bottom left). Conversely, ResNet-18 attains the best coverage on image tasks, and coverage is roughly similar between ResNet-18, PCA, and raw features on diverse and text tasks. From this analysis, we conclude that **CLIP usage can hurt coverage.**

4.4 Ablation study of Snuba

We conclude our analyses with an ablation study of Snuba, the best performing AutoWS method that we evaluated. We consider the effects of varying the cardinality (the number of features that each LF can consider), the LF selection criterion used by Snuba (F1 score), and the effect of increasing the initial number of labels beyond the original 100.

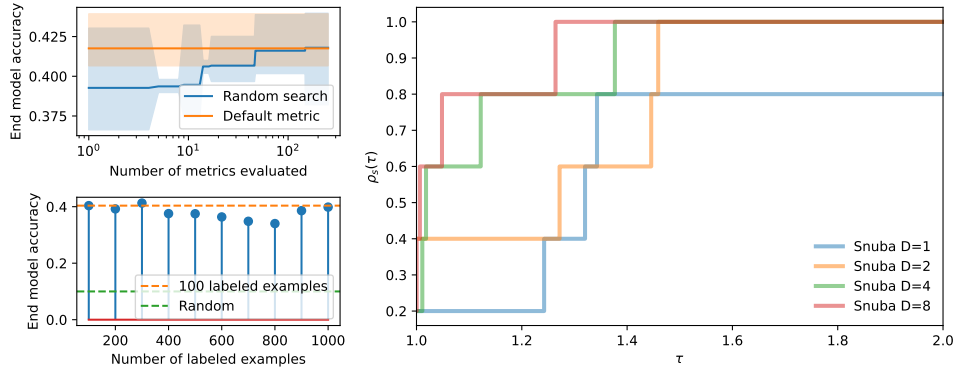


Figure 5: (Top left) Tuning Snuba’s LF selection and abstention criteria do not lead to an improvement on MNIST. Results are reported as averages, minima, and maxima over 3 random seeds. We evaluate Snuba on MNIST using PCA and 500 feature combination samples with cardinality $D = 2$. (Bottom left) Increasing the number of labeled examples does not improve the performance of Snuba. (Right) Increasing cardinality can lead to some improvement with Snuba.

Does increasing cardinality help Snuba? Snuba’s cardinality parameter dictates how many components of the feature representation each LF can consider during its LF synthesis procedure. We evaluate the aggregate effect on performance of varying this parameter using performance profiles, as shown in Figure 5 (left). In this case, we set S to be Snuba with cardinalities $D = 1, 2, 4,$ and 8 . We consider only CLIP embeddings and all datasets on which CLIP is applicable: MNIST, CIFAR-10, Spherical MNIST, Permuted MNIST, and Navier-Stokes. This limits the maximum cardinality that we can consider to 10, which allows us to explore the full space of possible improvements for Snuba along the axis of cardinality. In these settings, increasing cardinality improves performance up to a point. Beyond $D = 4$, we observe that Snuba ceases to improve much. From this, we conclude that **increasing cardinality can lead to performance improvements up to a point**.

Is F1 the right metric for MNIST when using Snuba? Given the poor performance of Snuba on MNIST, we evaluate Snuba’s default choice to use F1 scores for LF selection and for determining abstain thresholds—micro F1 and weighted F1, respectively. We do so by first defining a search space over all applicable classification metrics available in scikit-learn [47]. These include Snuba’s default choices, accuracy, balanced accuracy, precision, recall, Cohen’s kappa coefficient, Jaccard index, Matthews correlation coefficient, and using the micro-averaged F1 score for both LF selection and to determine abstain thresholds. We perform a random search over convex combinations of these 9 metrics by sampling configurations from a Dirichlet distribution with parameter $\alpha = \mathbf{1}_9$. As shown in Figure 5, we find no appreciable improvement over the default configuration. However, the best configuration found by random search has majority weight on micro-averaged F1 score, which only slightly differs from the default configuration in Snuba. These results indicate that **Snuba’s poor performance on MNIST is not trivially due to a poor choice of metric for LF selection**.

Do more labels help Snuba? We ask if we can further improve performance on MNIST by increasing the number of labeled examples. In this experiment, we varied the number of labeled examples given to Snuba from 100 to 1000. We set the cardinality to $D = 2$ and use raw pixel features. For efficiency, we randomly subsample 1000 feature combinations so as to avoid exploring the entire space of pairwise feature combinations. We answer the question in the negative: our results in Figure 5 show that increasing the number of labeled examples does not improve the performance of Snuba. This suggests that **any performance with Snuba in this setting is likely algorithmic, and not due to a lack of labeled examples**.

5 Conclusion

In this work, we proposed AutoWS-Bench-101, a benchmarking framework for AutoWS methods and beyond on a diverse set of classification tasks. We found that foundation models can improve the performance of AutoWS methods on in-distribution tasks but they can also hurt coverage, sometimes dramatically, on out-of-distribution tasks. We furthermore found that AutoWS methods using multipolar LFs might outperform unipolar LFs on average, but can result in lower coverage as the number of classes increases. One limitation is that we only considered CLIP—but there are many other applicable methods to be studied in future work. We hope this work takes a first step towards understanding how to build best-of-all-worlds automated weak supervision.

References

- [1] A. Ratner, C. D. Sa, S. Wu, D. Selsam, and C. Ré, “Data programming: Creating large training sets, quickly,” in *Proceedings of the 30th International Conference on Neural Information Processing Systems, NIPS’16*, (Red Hook, NY, USA), p. 3574–3582, Curran Associates Inc., 2016.
- [2] A. J. Ratner, S. H. Bach, H. R. Ehrenberg, J. A. Fries, S. Wu, and C. Ré, “Snorkel: Rapid training data creation with weak supervision,” *Proceedings of the VLDB Endowment. International Conference on Very Large Data Bases*, vol. 11 3, pp. 269–282, 2017.
- [3] A. J. Ratner, B. Hancock, J. Dunnmon, F. Sala, S. Pandey, and C. Ré, “Training complex models with multi-task weak supervision,” in *Proceedings of the AAAI Conference on Artificial Intelligence*, (Honolulu, Hawaii), 2019.
- [4] D. Y. Fu, M. F. Chen, F. Sala, S. M. Hooper, K. Fatahalian, and C. Ré, “Fast and three-rious: Speeding up weak supervision with triplet methods,” in *Proceedings of the 37th International Conference on Machine Learning (ICML 2020)*, 2020.
- [5] J. A. Dunnmon, A. J. Ratner, K. Saab, N. Khandwala, M. Markert, H. Sagreiya, R. Goldman, C. Lee-Messer, M. P. Lungren, D. L. Rubin, and C. Ré, “Cross-modal data programming enables rapid medical machine learning.,” *Patterns (N Y)*, vol. 1, May 2020.
- [6] J. A. Fries, P. Varma, V. S. Chen, K. Xiao, H. Tejada, P. Saha, J. Dunnmon, H. Chubb, S. Maskatia, M. Fiterau, S. Delp, E. Ashley, C. Ré, and J. R. Priest, “Weakly supervised classification of aortic valve malformations using unlabeled cardiac mri sequences,” *Nature Communications*, vol. 10, no. 1, p. 3111, 2019.
- [7] C. Sudlow, J. Gallacher, N. Allen, V. Beral, P. Burton, J. Danesh, P. Downey, P. Elliott, J. Green, M. Landray, B. Liu, P. Matthews, G. Ong, J. Pell, A. Silman, A. Young, T. Sprosen, T. Peakman, and R. Collins, “Uk biobank: an open access resource for identifying the causes of a wide range of complex diseases of middle and old age.,” *PLoS Med*, vol. 12, p. e1001779, Mar 2015.
- [8] S. H. Bach, D. Rodriguez, Y. Liu, C. Luo, H. Shao, C. Xia, S. Sen, A. Ratner, B. Hancock, H. Alborzi, *et al.*, “Snorkel drybell: A case study in deploying weak supervision at industrial scale,” in *Proceedings of the 2019 International Conference on Management of Data*, pp. 362–375, 2019.
- [9] C. Ré, F. Niu, P. Gudipati, and C. Srisuwananukorn, “Overton: A data system for monitoring and improving machine-learned products,” in *Proceedings of the 10th Annual Conference on Innovative Data Systems Research*, 2020.
- [10] S. Hooper, M. Wornow, Y. H. Seah, P. Kellman, H. Xue, F. Sala, C. Langlotz, and C. Re, “Cut out the annotator, keep the cutout: better segmentation with weak supervision,” in *International Conference on Learning Representations*, 2021.
- [11] C. Shin, W. Li, H. Vishwakarma, N. C. Roberts, and F. Sala, “Universalizing weak supervision,” in *International Conference on Learning Representations (ICLR)*, 2022.
- [12] P. Varma and C. Ré, “Snuba: Automating weak supervision to label training data,” *Proc. VLDB Endow.*, vol. 12, p. 223–236, nov 2018.
- [13] B. Boecking, W. Neiswanger, E. Xing, and A. Dubrawski, “Interactive weak supervision: Learning useful heuristics for data labeling,” in *International Conference on Learning Representations (ICLR)*, 2021.
- [14] N. Das, S. Chaba, R. Wu, S. Gandhi, D. H. Chau, and X. Chu, “Goggles: Automatic image labeling with affinity coding,” in *Proceedings of the 2020 ACM SIGMOD International Conference on Management of Data, SIGMOD ’20*, (New York, NY, USA), p. 1717–1732, Association for Computing Machinery, 2020.
- [15] M. Chen, D. Fu, D. Adila, M. Zhang, F. Sala, K. Fatahalian, and C. Ré, “Shoring up the foundations: Fusing model embeddings and weak supervision,” in *Uncertainty in Artificial Intelligence (UAI)*, 2022.
- [16] R. Smith, J. A. Fries, B. Hancock, and S. H. Bach, “Language models in the loop: Incorporating prompting into weak supervision,” 2022.
- [17] A. Radford, J. W. Kim, C. Hallacy, A. Ramesh, G. Goh, S. Agarwal, G. Sastry, A. Askell, P. Mishkin, J. Clark, *et al.*, “Learning transferable visual models from natural language supervision,” in *International Conference on Machine Learning*, pp. 8748–8763, PMLR, 2021.

- [18] T. Brown, B. Mann, N. Ryder, M. Subbiah, J. D. Kaplan, P. Dhariwal, A. Neelakantan, P. Shyam, G. Sastry, A. Askell, S. Agarwal, A. Herbert-Voss, G. Krueger, T. Henighan, R. Child, A. Ramesh, D. Ziegler, J. Wu, C. Winter, C. Hesse, M. Chen, E. Sigler, M. Litwin, S. Gray, B. Chess, J. Clark, C. Berner, S. McCandlish, A. Radford, I. Sutskever, and D. Amodei, “Language models are few-shot learners,” in *Advances in Neural Information Processing Systems*, 2020.
- [19] V. Sanh, A. Webson, C. Raffel, S. H. Bach, L. Sutawika, Z. Alyafeai, A. Chaffin, A. Stiegler, T. L. Scao, A. Raja, M. Dey, M. S. Bari, C. Xu, U. Thakker, S. S. Sharma, E. Szczechla, T. Kim, G. Chhablani, N. Nayak, D. Datta, J. Chang, M. T.-J. Jiang, H. Wang, M. Manica, S. Shen, Z. X. Yong, H. Pandey, R. Bawden, T. Wang, T. Neeraj, J. Rozen, A. Sharma, A. Santilli, T. Fevry, J. A. Fries, R. Teehan, S. Biderman, L. Gao, T. Bers, T. Wolf, and A. M. Rush, “Multitask prompted training enables zero-shot task generalization,” in *International Conference on Learning Representations (ICLR)*, 2022.
- [20] J. Zhang, Y. Yu, Y. Li, Y. Wang, Y. Yang, M. Yang, and A. Ratner, “WRENCH: A comprehensive benchmark for weak supervision,” in *Thirty-fifth Conference on Neural Information Processing Systems Datasets and Benchmarks Track (Round 2)*, 2021.
- [21] S. Gupta and C. Manning, “Improved pattern learning for bootstrapped entity extraction,” in *Proceedings of the Eighteenth Conference on Computational Natural Language Learning*, pp. 98–108, 2014.
- [22] D. R. Karger, S. Oh, and D. Shah, “Iterative learning for reliable crowdsourcing systems,” in *Advances in neural information processing systems*, pp. 1953–1961, 2011.
- [23] A. P. Dawid and A. M. Skene, “Maximum likelihood estimation of observer error-rates using the EM algorithm,” *Applied statistics*, pp. 20–28, 1979.
- [24] M. Mintz, S. Bills, R. Snow, and D. Jurafsky, “Distant supervision for relation extraction without labeled data,” in *Proceedings of the Joint Conference of the 47th Annual Meeting of the ACL and the 4th International Joint Conference on Natural Language Processing of the AFNLP: Volume 2-Volume 2*, pp. 1003–1011, Association for Computational Linguistics, 2009.
- [25] M. A. Hearst, “Automatic acquisition of hyponyms from large text corpora,” in *Proceedings of the 14th conference on Computational linguistics-Volume 2*, pp. 539–545, Association for Computational Linguistics, 1992.
- [26] S. Galhotra, B. Golshan, and W.-C. Tan, “Adaptive rule discovery for labeling text data,” in *Proceedings of the 2021 International Conference on Management of Data, SIGMOD ’21*, (New York, NY, USA), p. 2217–2225, Association for Computing Machinery, 2021.
- [27] R. Zhang, Y. Yu, P. Shetty, L. Song, and C. Zhang, “Prompt-based rule discovery and boosting for interactive weakly-supervised learning,” in *Proceedings of the 60th Annual Meeting of the Association for Computational Linguistics (Volume 1: Long Papers)*, (Dublin, Ireland), pp. 745–758, Association for Computational Linguistics, May 2022.
- [28] C.-Y. Hsieh, J. Zhang, and A. Ratner, “Nemo: Guiding and contextualizing weak supervision for interactive data programming,” 2022.
- [29] R. Pryzant, Z. Yang, Y. Xu, C. Zhu, and M. Zeng, “Automatic rule induction for efficient semi-supervised learning,” 2022.
- [30] K. He, X. Zhang, S. Ren, and J. Sun, “Deep residual learning for image recognition,” in *2016 IEEE Conference on Computer Vision and Pattern Recognition (CVPR)*, pp. 770–778, 2016.
- [31] T. Chen, S. Kornblith, M. Norouzi, and G. Hinton, “A simple framework for contrastive learning of visual representations,” in *Proceedings of the 37th International Conference on Machine Learning* (H. D. III and A. Singh, eds.), vol. 119 of *Proceedings of Machine Learning Research*, pp. 1597–1607, PMLR, 13–18 Jul 2020.
- [32] J.-B. Grill, F. Strub, F. Altché, C. Tallec, *et al.*, “Bootstrap your own latent a new approach to self-supervised learning,” in *Advances in Neural Information Processing Systems (NeurIPS)*, 2020.
- [33] R. Bommasani, D. A. Hudson, E. Adeli, R. Altman, S. Arora, *et al.*, “On the opportunities and risks of foundation models.” <https://arxiv.org/abs/2108.07258>, 2021.
- [34] L. Deng, “The mnist database of handwritten digit images for machine learning research [best of the web],” *IEEE Signal Processing Magazine*, vol. 29, no. 6, pp. 141–142, 2012.

- [35] A. Krizhevsky, V. Nair, and G. Hinton, “Cifar-10 (canadian institute for advanced research),”
- [36] T. S. Cohen, M. Geiger, J. Köhler, and M. Welling, “Spherical CNNs,” in *International Conference on Learning Representations (ICLR)*, 2018.
- [37] T. C. Alberto, J. V. Lochter, and T. A. Almeida, “Tubespam: Comment spam filtering on youtube,” in *2015 IEEE 14th International Conference on Machine Learning and Applications (ICMLA)*, pp. 138–143, 2015.
- [38] X. Zhang, J. Zhao, and Y. LeCun, “Character-level convolutional networks for text classification,” in *Advances in Neural Information Processing Systems* (C. Cortes, N. Lawrence, D. Lee, M. Sugiyama, and R. Garnett, eds.), vol. 28, Curran Associates, Inc., 2015.
- [39] W. Ren, Y. Li, H. Su, D. Kartchner, C. Mitchell, and C. Zhang, “Denoising multi-source weak supervision for neural text classification,” in *Findings of the Association for Computational Linguistics: EMNLP 2020*, (Online), pp. 3739–3754, Association for Computational Linguistics, Nov. 2020.
- [40] A. L. Maas, R. E. Daly, P. T. Pham, D. Huang, A. Y. Ng, and C. Potts, “Learning word vectors for sentiment analysis,” in *Proceedings of the 49th Annual Meeting of the Association for Computational Linguistics: Human Language Technologies*, (Portland, Oregon, USA), pp. 142–150, Association for Computational Linguistics, June 2011.
- [41] G. D. Clifford, C. Liu, B. Moody, L.-w. H. Lehman, I. Silva, Q. Li, A. E. Johnson, and R. G. Mark, “Af classification from a short single lead ecg recording: The physionet/computing in cardiology challenge 2017,” in *2017 Computing in Cardiology (CinC)*, pp. 1–4, 2017.
- [42] Z. Li, N. B. Kovachki, K. Azizzadenesheli, B. liu, K. Bhattacharya, A. Stuart, and A. Anandkumar, “Fourier neural operator for parametric partial differential equations,” in *International Conference on Learning Representations (ICLR)*, 2021.
- [43] H. S. Anderson and P. Roth, “EMBER: an open dataset for training static PE malware machine learning models,” *CoRR*, vol. abs/1804.04637, 2018.
- [44] F. Wang and C. Zhang, “Label propagation through linear neighborhoods,” *IEEE Transactions on Knowledge and Data Engineering*, vol. 20, no. 1, pp. 55–67, 2008.
- [45] E. D. Dolan and J. J. Moré, “Benchmarking optimization software with performance profiles,” *Mathematical Programming*, vol. 91, no. 2, pp. 201–213, 2002.
- [46] I. Papadimitriou and D. Jurafsky, “Learning Music Helps You Read: Using transfer to study linguistic structure in language models,” in *Proceedings of the 2020 Conference on Empirical Methods in Natural Language Processing (EMNLP)*, (Online), pp. 6829–6839, Association for Computational Linguistics, Nov. 2020.
- [47] F. Pedregosa, G. Varoquaux, A. Gramfort, V. Michel, B. Thirion, O. Grisel, M. Blondel, P. Prettenhofer, R. Weiss, V. Dubourg, J. Vanderplas, A. Passos, D. Cournapeau, M. Brucher, M. Perrot, and E. Duchesnay, “Scikit-learn: Machine learning in Python,” *Journal of Machine Learning Research*, vol. 12, pp. 2825–2830, 2011.

Appendix

The appendix is organized as follows. First, we will detail the licenses for the datasets that are part of our benchmark. Second, we will provide additional insights that AutoWS-Bench-101 generated. These include a study of coverage for our techniques. We then perform additional ablations for GOGGLES and IWS. We also compare AutoWS with hand-crafted LFs, confirming that there are significant improvements available in cases where manual LFs are noisy. Next, we provide experimental details including the prompts that we used for our zero-shot CLIP experiments. Finally, we provide additional explanations of the incompatibilities between various methods in our pipeline. We conclude with societal and privacy implications for this work.

A Dataset licenses

The license information is provided below.

- **MNIST:** CC BY-SA 3.0
- **CIFAR-10:** CC BY 4.0 (on <https://www.tensorflow.org/datasets/catalog/cifar10>)
- **Spherical MNIST:** MIT
- **Permuted MNIST:** Apache 2.0
- **Navier-Stokes:** MIT
- **ECG:** ODC-BY 1.0
- **EMBER:** MIT
- **YouTube:** Apache 2.0
- **Yelp:** https://s3-media0.fl.yelpcdn.com/assets/srv0/engineering_pages/dclcabe7cb95/assets/vendor/Dataset_User_Agreement.pdf
- **IMDb:** https://www.imdb.com/conditions?pf_rd_m=A2FGELUUNOQJNL&pf_rd_p=3aefe545-f8d3-4562&pf_rd_r=FP5VRV15YGQSTMJVFZDM&pf_rd_s=center-1&pf_rd_t=60601&pf_rd_i=interfaces&ref_=fea_mn_1k2

B Coverage analysis

Table 2 provides the results for coverage (the percentage of points in the dataset that get labeled) for the techniques we studied. We note that Snuba often produces relatively high coverage, especially with PCA-based feature representations.

	MNIST	CIFAR-10	SPHERICAL MNIST	PERMUTED MNIST	ECG	NAVIER-STOKES	EMBER	YOUTUBE	YELP	IMDb
IWS										
+RAW FEATURES	0.3617	0.4616	0.3666	0.3656	0.5125	0.8163	1.0000	0.9640	1.0000	0.7908
+PCA	0.5107	0.2731	0.2696	0.4797	0.5448	0.9874	0.8873	0.9200	0.9616	0.9816
+RESNET-18	0.7422	0.3580	0.0917	0.1631	0.6109	1.0000	0.6142	1.0000	0.6368	0.8596
+CLIP	0.2758	0.7239	0.0993	0.1757	N/A	N/A	N/A	N/A	N/A	N/A
SNUBA										
+RAW FEATURES	0.6842	0.6409	0.8387	0.8105	0.9090	0.5379	1.0000	1.0000	1.0000	1.0000
+PCA	0.9608	0.7183	0.9557	0.9716	0.9956	1.0000	0.8072	1.0000	0.9971	1.0000
+RESNET-18	0.8761	0.9772	0.9230	0.9320	0.8998	1.0000	0.5912	1.0000	0.9884	1.0000
+CLIP	0.7667	0.7262	0.1521	0.1323	N/A	0.4116	N/A	1.0000	0.4781	0.2716
SNUBA (MULTIPOLAR)										
+RAW FEATURES	0.7422	0.8129	0.4470	0.5407	1.0000	1.0000	1.0000	1.0000	1.0000	1.0000
+PCA	0.3472	0.5807	0.4763	0.3472	1.0000	1.0000	1.0000	1.0000	1.0000	1.0000
+RESNET-18	0.6185	0.6337	0.8232	0.7193	1.0000	1.0000	1.0000	1.0000	1.0000	1.0000
+CLIP	0.5027	0.3372	0.2033	0.7235	N/A	1.0000	N/A	0.7320	0.5926	0.2816

Table 2: Coverage of AutoWS methods using various feature representations across datasets.

C Ablation study of GOGGLES

Next, we perform an ablation study of GOGGLES. In our analysis, we will evaluate three questions: whether GOGGLES improves when combining embedding types, how GOGGLES performs per-class, and whether or not the choice of inference model should be tuned.

Does GOGGLES improve with more embedding types? Instead of using a single type of feature representation to compute affinity scores between instance pairs, we leverage different types of embeddings to create multiple affinity matrices. These are then stacked and fed to the hierarchical generative model in GOGGLES for label inference. Through different types of embeddings, GOGGLES may capture correlations from different views. We evaluate the performance of GOGGLES with more embedding types in Table 3. Note that the ECG dataset and EMBER dataset use three types of embeddings only (they do not use CLIP embeddings) to create affinity matrices. Compared to the best single-embedding performance for each dataset in Table 1, we find that GOGGLES does not improve with more embedding types. Specifically, only on MNIST and EMBER is performance close to the single best embedding. We hypothesize that this is due to potentially poor alignment between these embeddings, and that with a more sophisticated approach, improvements versus single best are possible.

	MNIST	CIFAR-10	SPHERICAL MNIST	PERMUTED MNIST	ECG	NAVIER-STOKES	EMBER
GOGGLES							
MULTIPLE REPRESENTATIONS	0.425	0.2313	0.1072	0.4085	0.2767	0.4868	0.6728
BEST SINGLE REP. PERFORMANCE	0.4563	0.5436	0.1884	0.4561	0.3127	0.9353	0.6728

Table 3: Multiple types of feature representations for GOGGLES.

How does GOGGLES perform per-class? Next, we measured the per-class precision recall curves using GOGGLES. GOGGLES has perfect coverage on all tasks. However, we find that in several scenarios, the per-class performance varies considerably (e.g., MNIST, CIFAR-10).

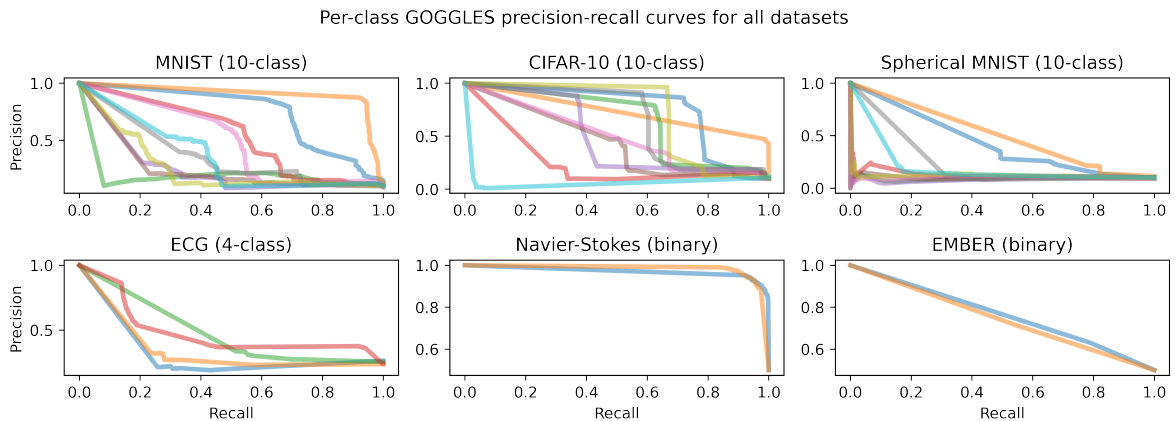


Figure 6: Class-wise precision recall curves using GOGGLES across datasets. Despite having 100% coverage on all tasks, GOGGLES has wildly varying per-class performance that becomes more pronounced as the number of classes increases. Permuted MNIST is not shown as the predictions are the same as on MNIST due to the permutation invariance of PCA.

Does GOGGLES improve with different clustering models? The default clustering model in GOGGLES is Gaussian mixture model (GMM). We also compare the performance of label inference with another two clustering models: K-means clustering and Spectral clustering. The input of the clustering model is the affinity matrix computed by cosine similarity scores between embeddings of each example. After we train clustering model and obtain clusters, GOGGLES use our 100 labeled examples to map clusters to classes. In Table 4, we see that GMM often outperforms the other clustering models on seven of the ten datasets. We conclude that GMM clustering is often good enough, but that a different cluster model might improve performance slightly.

	MNIST	CIFAR-10	SPHERICAL MNIST	PERMUTED MNIST	ECG	NAVIER-STOKES	EMBER	YOUTUBE	YELP	IMDB
GOGGLES (GMM)										
+RAW FEATURES	0.3778	0.1697	0.0897	0.3778	0.2710	0.5284	0.5283	0.5880	0.4732	0.5516
+PCA	0.4563	0.1989	0.1074	0.4561	0.2688	0.4863	0.6728	0.5880	0.5466	0.5628
+RESNET-18	0.3258	0.1768	0.1192	0.1894	0.3127	0.9353	0.5312	0.5200	0.4553	0.5152
+CLIP	0.3309	0.5436	0.1884	0.1405	N/A	0.7505	N/A	0.5280	0.4779	0.5000
GOGGLES (K-MEANS)										
+RAW FEATURES	0.3808	0.1416	0.1092	0.3808	0.2715	0.5226	0.5294	0.5320	0.4750	0.5344
+PCA	0.4099	0.1738	0.1136	0.3960	0.2672	0.4826	0.6720	0.5960	0.5413	0.5720
+RESNET-18	0.3294	0.1877	0.1112	0.2001	0.2814	0.9416	0.5296	0.5200	0.4574	0.5136
+CLIP	0.3730	0.5604	0.1342	0.1400	N/A	0.7063	N/A	0.5280	0.4779	0.5000
GOGGLES (SPECTRAL)										
+RAW FEATURES	0.0355	0.1006	0.0938	0.0355	0.2305	0.5142	0.5294	0.5320	0.4626	0.5308
+PCA	0.1308	0.1002	0.1033	0.0814	0.2356	0.4874	0.6639	0.6120	0.5413	0.4356
+RESNET-18	0.1541	0.1165	0.0705	0.1130	0.2383	0.9168	0.5249	0.5480	0.5405	0.5152
+CLIP	0.1923	0.0953	0.1130	0.1480	N/A	0.9858	N/A	0.5160	0.4779	0.4996

Table 4: Different clustering methods for GOGGLES.

D Ablation study of Interactive Weak Supervision

We perform an ablation study of IWS. In particular, we evaluate the effect of using IWS in its original interactive form using a human-in-the-loop against the automatic selection rule used in the rest of our experiments. We furthermore evaluate the effect of tuning the accuracy threshold parameter of the automatic selection rule.

Does Interactive Weak Supervision require a human-in-the-loop? We evaluate the effect of relying on the automatic selection rule of IWS as opposed to using the original human-in-the-loop during the LF selection process. We consider three datasets: MNIST, Navier-Stokes, and Yelp, each subject to using the highest performing embedding using IWS according to Table 1 (CLIP, ResNet-18, raw BERT features, respectively). In the human-in-the-loop setting, during each round of interaction, we prompt the user with a set of several scores: coverage, precision, recall, and accuracy, each computed on the validation set of 100 labels. Given this information, we ask whether or not the LF should be used. We find that on MNIST, the human-in-the-loop procedure results in very similar accuracies and coverage scores to that of the automated procedure. On Navier-Stokes, however, the human-in-the-loop procedure results in much higher accuracy while retaining the perfect coverage of the automated procedure. Finally, on Yelp, the human-in-the-loop procedure actually worsens performance and significantly reduces coverage. We postulate that this is because the difficulty of estimating the quality of the synthesized LFs varies considerably dataset-to-dataset, given these scores. It is furthermore not always clear that using a similar strategy to that of the automated procedure is the best strategy. From this analysis, we conclude that a practitioner should consider trying the human-in-the-loop procedure, but does not necessarily guarantee improved results over the automated procedure.

	MNIST + CLIP	NAVIER-STOKES + RESNET-18	YELP + RAW FEATURES
HUMAN-IN-THE-LOOP	0.6826 (0.2766)	0.9753 (1.0000)	0.5675 (0.5377)
AUTOMATIC	0.6885 (0.2758)	0.7995 (1.0000)	0.6034 (1.0000)

Table 5: The automatic selection rule used in IWS leads to improved accuracy and coverage over its human-in-the-loop counterpart on MNIST, Navier-Stokes, and Yelp. Results are presented in the form of “accuracy (coverage)” pairs.

Does the automatic selection rule of Interactive Weak Supervision require tuning? We compare the effect of tuning the accuracy threshold used to automatically select LFs when using IWS under its automatic settings (i.e., without a human-in-the-loop). We perform this analysis using the same data settings as in the previous analysis: MNIST with CLIP features, Navier-Stokes with ResNet-18 features, and Yelp with raw features (BERT). We present these results in Figure 7. We find that tuning this threshold parameter does not improve performance by much, if at all—and if the accuracy threshold parameter is set to be too large, then coverage can drop, as is the case for Navier-Stokes and Yelp (see Figure 7 center and right). In the case of MNIST, this parameter had essentially no impact on accuracy or coverage.

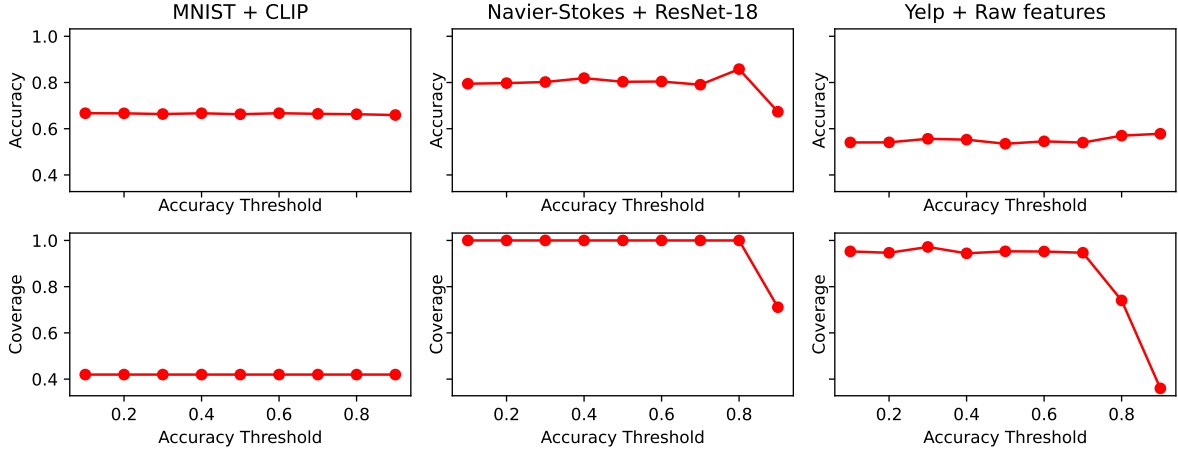


Figure 7: Tuning the threshold parameter of the automated version of IWS does not lead to significant improvements in performance, and can hurt coverage if it is set to be too high.

	GOLD	HUMAN LFS	SNUBA LFS	HUMAN LFS + SNUBA LFS
F1 SCORE	64.97	43.18	62.55	61.39

Table 6: Comparison between Snuba and hand-designed LFs on the Basketball dataset.

E Comparison to hand-designed LFs

So far, all of our results have looked at various flavors of AutoWS, and, in addition, examined few-/zero-shot capable models like CLIP. A natural question is whether AutoWS is competitive against manual WS. Indeed, this is the original motivation for AutoWS methods. This question is challenging to benchmark, since it is a function of the quality of the LFs. For example, a perfectly accurate manually-written LF cannot be improved upon. Instead, we provide a simple proof-of-concept.

We compare against a set of pre-existing manually-written LFs from [4] for the basketball dataset. These were also used as part of the WRENCH [20] benchmark. We then ran SNUBA on the dataset using our standard configuration. We found that SNUBA performs nearly as well as the gold (supervised) setting, while the human LFs are nearly 20 points worse. An additional question is whether SNUBA-generated LFs combine well with manual LFs. While this is a promising direction for future research, simply including both sets of LFs did not outperform the automatically generated ones.

F CLIP Zero-shot Prompts

We provide the prompts that we used with CLIP.

Dataset	Prompt
MNIST	"a photo of the number: "[label]"."
CIFAR-10	"a photo of a [label]."
Spherical MNIST	"a photo of the number: "[label]" stereographically projected onto a sphere and back to the plane."
Permuted MNIST	"a photo of the number: "[label]" permuted by a bit reversal permutation."
Navier-Stokes	["The Navier-Stokes equation in the turbulent regime with low viscosity: 1e-5.", "The Navier-Stokes equation with high viscosity: 1e-3."]
YouTube	["Ham", "Spam"]
Yelp	["Negative", "Positive"]
IMDb	["Negative", "Positive"]

Table 7: Prompts used to get zero-shot CLIP embedding

G Incompatibilities between methods, feature representations, and tasks

As noted in Table 1, several methods, feature representations, and tasks are incompatible, resulting in several missing entries denoted as N/A. Here, we itemize and elaborate on the reasons for each missing entry.

- **CLIP features and ECG:** CLIP does not support ECG as it comprises time-series vectors.
- **CLIP features and Ember:** CLIP does not support Ember as it comprises feature vectors.
- **CLIP features and IWS on binary classification tasks:** For binary classification tasks, CLIP produces feature vectors with only two entries corresponding to its per-class logits. This only allows for a small handful of LFs to be generated. However, in this case, IWS requires more LFs than can be generated from this two-dimensional logits vector while still using the same procedure used elsewhere. This limitation applies to Navier-Stokes, YouTube, Yelp, and IMDb, as they are all binary classification tasks.